ARTICLE

Thoracic perivascular adipose tissue inhibits VSMC apoptosis and aortic aneurysm formation in mice via the secretome of browning adipocytes

Chun-ling Huang[1], Yu-na Huang[2], Lei Yao[1], Jun-ping Li[2], Zeng-hui Zhang[2], Zhao-qi Huang[2], Si-xu Chen[2], Yu-ling Zhang[2], Jing-feng Wang[2], Yang-xin Chen[2] and Zhao-yu Liu[1]

Abdominal aortic aneurysm (AAA) is a dangerous vascular disease without any effective drug therapies so far. Emerging evidence suggests the phenotypic differences in perivascular adipose tissue (PVAT) between regions of the aorta are implicated in the development of atherosclerosis evidenced by the abdominal aorta more vulnerable to atherosclerosis than the thoracic aorta in large animals and humans. The prevalence of thoracic aortic aneurysms (TAA) is much less than that of abdominal aortic aneurysms (AAA). In this study we investigated the effect of thoracic PVAT (T-PVAT) transplantation on aortic aneurysm formation and the impact of T-PVAT on vascular smooth muscle cells. Calcium phosphate-induced mouse AAA model was established. T-PVAT (20 mg) was implanted around the abdominal aorta of recipient mice after removal of endogenous abdominal PVAT (A-PVAT) and calcium phosphate treatment. Mice were sacrificed two weeks after the surgery and the maximum external diameter of infrarenal aorta was measured. We found that T-PVAT displayed a more BAT-like phenotype than A-PVAT; transplantation of T-PVAT significantly attenuated calcium phosphate-induced abdominal aortic dilation and elastic degradation as compared to sham control or A-PVAT transplantation. In addition, T-PVAT transplantation largely preserved smooth muscle cell content in the abdominal aortic wall. Co-culture of T-PVAT with vascular smooth muscle cells (VSMCs) significantly inhibited H_2O_2- or TNFα plus cycloheximide-induced VSMC apoptosis. RNA sequencing analysis showed that T-PVAT was enriched by browning adipocytes and anti-apoptotic secretory proteins. We further verified that the secretome of mature adipocytes isolated from T-PVAT significantly inhibited H_2O_2- or TNFα plus cycloheximide-induced VSMC apoptosis. Using proteomic and bioinformatic analyses we identified cartilage oligomeric matrix protein (COMP) as a secreted protein significantly increased in T-PVAT. Recombinant COMP protein significantly inhibited VSMC apoptosis. We conclude that T-PVAT exerts anti-apoptosis effect on VSMCs and attenuates AAA formation, which is possibly attributed to the secretome of browning adipocytes.

Keywords: abdominal aortic aneurysm; perivascular adipose tissue; browning; vascular smooth muscle cells; apoptosis; secretome

INTRODUCTION

Abdominal aortic aneurysm (AAA) is a permanent focal dilation of the abdominal aorta which can lead to sudden death due to aortic rupture. AAA causes over 175,000 deaths per year worldwide [1]. Currently no effective pharmacological therapies have been identified. Therefore, new mechanisms and new strategies are urgently to be explored.

Perivascular adipose tissue (PVAT) is a unique adipose tissue surrounding the vasculature and has been shown to contribute to vascular homeostasis and pathology [2]. Studies have demonstrated that PVAT can regulate the contractile ability of blood vessels and further the development of hypertension [3–5]. In addition, PVAT is involved in the proliferation and migration of vascular smooth muscle cells (VSMCs), secretion of adipokines and cytokines, and thus participates in the progression of neointima hyperplasia and atherosclerosis [6–9]. Recently, PVAT has also been implicated in AAA pathophysiology, possibly through inflammatory gene expression and adipokines secretion [10–12].

Recently, it has been recognized that PVAT surrounding different regions of aorta is different. The phenotypic differences in PVAT between regions of the aorta have been implicated in the development of atherosclerosis as the evidence showed that the abdominal aorta is more vulnerable to atherosclerosis than the thoracic aorta in large animals and humans [13]. The prevalence of thoracic aortic aneurysms (TAA) is much less than that of abdominal aortic aneurysms (AAA) [14]. The average growth rate of TAA is also lower than AAA, with 0.1–0.2 cm/year

[1]Medical Research Center, Guangdong Provincial Key Laboratory of Malignant Tumor Epigenetics and Gene Regulation, Sun Yat-Sen Memorial Hospital, Sun Yat-Sen University, Guangzhou 510120, China and [2]Department of Cardiology, Guangdong Provincial Key Laboratory of Arrhythmia and Electrophysiology, Sun Yat-Sen Memorial Hospital, Sun Yat-Sen University, Guangzhou 510120, China
Correspondence: Jing-feng Wang (dr_wjf@vip.163.com) or Yang-xin Chen (chenyx39@mail.sysu.edu.cn) or Zhao-yu Liu (liuzhy98@mail.sysu.edu.cn)
These authors contributed equally: Chun-ling Huang, Yu-na Huang, Lei Yao

346

compared to 0.2–0.3 cm/year [15], suggesting that thoracic PVAT (T-PVAT) might exert a protective role in aortic aneurysm formation. Hereto, we investigated the effect of T-PVAT transplantation on aortic aneurysm formation and the impact of T-PVAT on vascular smooth muscle cells.

MATERIALS AND METHODS

Mouse model of calcium phosphate-induced AAA

Calcium phosphate-induced mouse AAA model was generated using 8-week-old male C57BL/6 mice purchased from Guangdong Medical Laboratory Animal Center and the surgery was performed as previously described [16]. Briefly, the infrarenal region of the abdominal aorta was isolated. A small piece of gauze soaked in 0.5 M CaCl$_2$ was applied perivascularly for 10 min and then replaced with another piece of PBS-soaked gauze for 5 min. Mice were sacrificed 2 weeks after the surgery and the maximum external diameter of infrarenal aorta was measured. All procedures performed were reviewed and approved by the Animal Care and Use Committee at Sun Yat-sen University.

Perivascular adipose tissue transplantation

The adipose tissue transplantation was performed as described previously [17]. Specifically, perivascular adipose tissue was isolated from C57BL/6 J mice and placed in Dulbecco's modified Eagle's medium (DMEM, Gibco, Thermo Fisher Scientific, Waltham, MA, USA) containing 10% fetal bovine serum (FBS) and 1% penicillin/streptomycin (P/S). Then 20 mg of perivascular adipose tissue was implanted around the abdominal aorta of recipient mice after removal of endogenous abdominal PVAT and calcium phosphate treatment.

Histology and immunostaining

The abdominal aorta was harvested and cut at the site of maximal diameter, and embedded in OCT for cross section preparation. Aortic sections (8 μm each) were collected serially from the proximal to the distal aorta and stained with hematoxylin and eosin (H&E). At least 3 measurements of the maximal expanded portion of the infrarenal aorta of each mouse were averaged before calculating the mean of each experimental group. Elastica van Gieson (EVG) staining, Sirius red staining and TUNEL staining were performed using Elastica van Gieson staining kit (Sigma, Burlington, MA, USA), Sirius red staining kit (Phyton Biotech, Delta, British Columbia, Canada) and One Step TUNEL Apoptosis Assay Kit (Beyotime, Shanghai, China), respectively. Elastin degradation was quantified as: 1, no elastin degradation; 2, mild degradation; 3, moderate; 4, moderate to severe; 5, severe elastin degradation. For immunostaining, primary antibodies against cleaved-caspase 3 (CST, Danvers, MA, USA) and smooth muscle alpha actin (GeneTex, Irvine, CA, USA) were used. Quantification of staining was performed using ImageJ Software.

Cell culture

Human aortic smooth muscle cells (HASMCs) were purchased from Sunncell Biotech (Wuhan, China) and maintained in smooth muscle cell medium (FineTest, Wuhan, China) under 5% CO$_2$ at 37 °C. Cells have been verified by smooth muscle alpha actin antibody staining and cells between passage 5 to 7 were used. At 80% confluency, cells were cultured with 20 mg PVAT or the culture medium of adipocytes or stromal vascular fraction (SVF) isolated from 20 mg PVAT for 24 h before apoptosis stimulant treatment.

Western blot analysis

Aortic tissues or cells were lysed by RIPA buffer (Beyotime, Shanghai, China) containing protease inhibitors and phosphatase inhibitors. Equal amounts of proteins from each group were separated by SDS-PAGE and transferred to PVDF membranes. The membranes were incubated with primary antibodies at 4 °C overnight and secondary antibodies for 1 h. Primary antibodies including anti-cleaved-caspase 3, anti-cleaved Parp and anti-GAPDH were purchased from CST (Danvers, MA, USA); Anti-UCP-1 was from Abcam (Cambridge, UK), anti-actin was from Santa Cruz (Dallas, TX, USA).

Annexin V apoptosis analysis

After being treated with 400 μM H$_2$O$_2$ for 24 h or 50 ng/mL TNFα plus 5 μg/mL cycloheximide (CHX) for 8 h, HASMCs were dissociated with 0.25% trypsin and stained with Annexin V Apoptosis Detection Kit (KeyGEN, Nanjing, China). In brief, the cells were washed with cold PBS, suspended in 1× binding buffer and stained with Annexin V-FITC and Propidium Iodide (PI). The flow cytometry analysis was performed by the flow cytometry core at the Medical Research Center of Sun Yat-sen Memorial Hospital and analyzed by FlowJo software.

Quantitative RT-PCR

RNA was extracted by TRIzol reagent (Invitrogen, Waltham, MA) according to the manufacturer's instructions. cDNA was synthesized using Hifair® II 1st Strand cDNA Synthesis Kit (Yeasen, Shanghai, China). Individual quantitative RT-PCR was performed using gene-specific primers as shown in Supplementary Table S1.

RNA-seq analysis

The RNA Libraries were sequenced with the Illumina HiSeq2000 (2 × 100 bp) performed by Guangzhou Ige BIOTECHNOLOGY Co. Ltd. Differentially expressed genes at a 5% false discovery rate (FDR) (adjusted P value ≤ 0.05) were identified. A functional annotation analysis of the differentially enriched pathway was performed using DAVID. Significantly enriched pathways were identified using a 5% FDR cutoff, and their enrichment significance was quantified using -log10 of adjusted P value.

Workflow for the prediction of secreted proteins

Putative secreted proteins were selected in three sets. From the total of the identified upregulated genes in T-PVAT, (1) those with predicted signal peptides by UniProt keyword annotation "Signal"; (2) those extracted by UniProt keyword annotation "Secreted"; (3) those with "extracellular locations" annotated by GO Cellular Component (GOCC). Finally, three sets were intersected together as the secreted proteins.

Statistical analysis

Data are presented as the means ± SEM. Statistical analyses were performed using Prism8 software (GraphPad). The statistical significance of differences between two groups was analyzed by Student's t tests. For comparing more than two means, one-way analysis of variance (ANOVA) with the Newman-Keuls post-hoc analysis was employed. Values of $P < 0.05$ were considered statistically significant.

RESULTS

T-PVAT exhibits a more BAT-like phenotype than A-PVAT

It has previously been reported that PVAT exhibits great regional variations along the aorta [13]. Here we first compared the histology between thoracic PVAT (T-PVAT) and abdominal PVAT (A-PVAT) in mice. T-PVAT was composed of multilocular adipocytes whereas A-PVAT was mainly composed of unilocular adipocytes, and the average adipocyte size was much smaller in T-PVAT than in A-PVAT (Fig. 1a, b). Uncoupling protein-1 (Ucp1), a classical browning marker, is highly expressed in T-PVAT but not in A-PVAT, as demonstrated by Western blotting
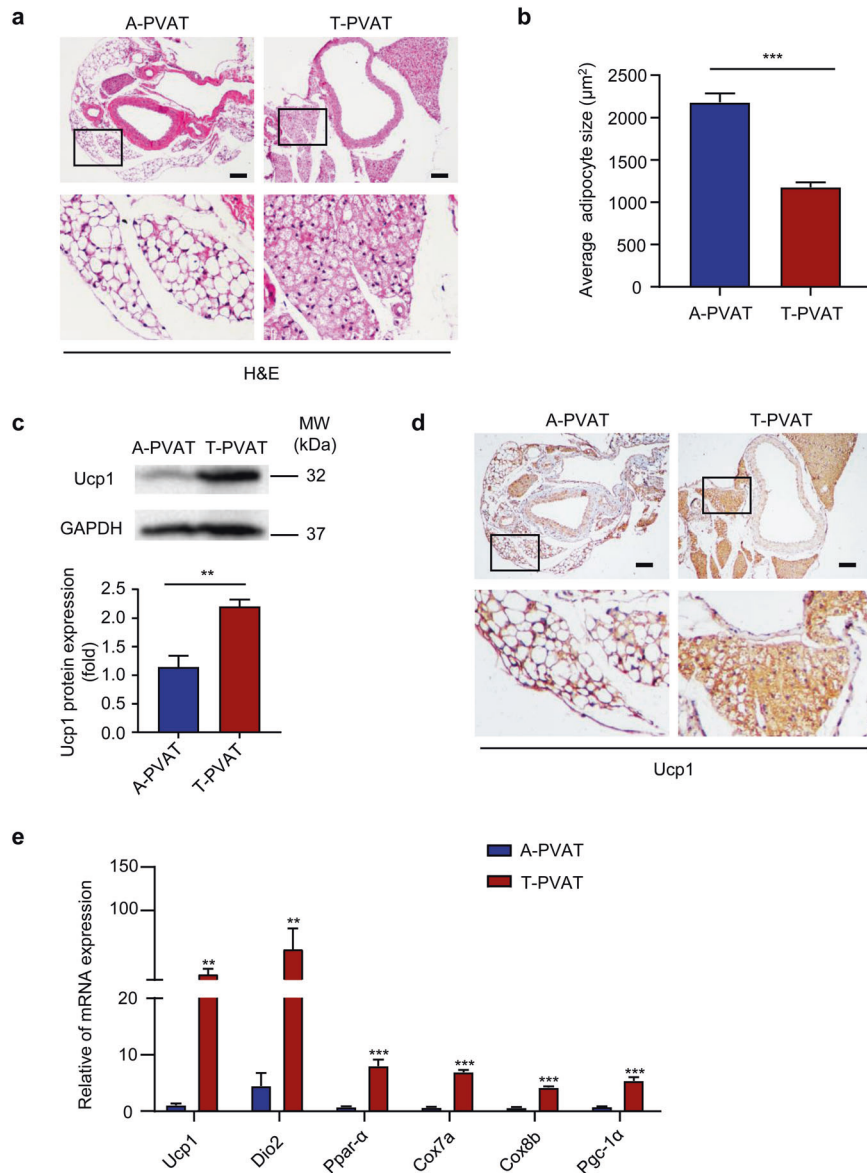
Thoracic PVAT attenuates aortic aneurysm formation
CL Huang et al.

347

Fig. 1 Thoracic PVAT (T-PVAT) exhibits a more BAT-like phenotype than abdominal PVAT (A-PVAT). a Hematoxylin and eosin (H&E) staining of A-PVAT and T-PVAT from C57/BL6 mice (Scale bar = 200 μm). **b** Average of adipocyte size. **c** Western blotting analysis of Ucp1. **d** Immunohistochemical staining of Ucp1. **e** Quantitative RT-PCR of browning markers ($n = 5$, **$P < 0.01$, ***$P < 0.001$).

and immunohistochemical staining (Fig. 1c, d). In addition, the mRNA expression of brown adipocyte markers such as Ucp1, Ppar-α, Cox7a, Cox8b and Pgc-1α are all significantly higher in T-PVAT than in A-PVAT (Fig. 1e). Together all these results suggest that T-PVAT exhibits a more BAT-like phenotype than A-PVAT.

Transplantation of T-PVAT attenuates abdominal aortic aneurysm formation
To investigate whether the change of PVAT around the abdominal aorta would impact AAA formation, we transplanted T-PVAT or A-PVAT onto the abdominal aorta of mice, which has undergone calcium phosphate treatment to induce AAA (Fig. 2a). Aortas treated with calcium phosphate showed a significant increase in aortic expansion after 14 days, compared with those treated with PBS. However, after T-PVAT transplantation, calcium phosphate-induced aortic expansion was significantly inhibited (Fig. 2b–d). H&E staining further revealed that T-PVAT

transplantation dramatically suppressed the expansion of the luminal region and thickening of the adventitia (Fig. 2e). These results suggest that transplantation of T-PVAT attenuates AAA formation.

Transplantation of T-PVAT attenuates medial elastin fragmentation and increases collagen deposition of the aortic wall
We further examined the elastic fiber integrity and collagen deposition of the abdominal aortic wall. Calcium phosphate strongly induced elastin fragmentation in sham group and A-PVAT transplantation group as revealed by EVG staining, whereas T-PVAT transplantation significantly lowered the severity of elastin fragmentation (Fig. 3a, c). Additionally, Sirius red staining revealed that T-PVAT transplantation dramatically increases the Sirius red positive area in the abdominal aortic wall (Fig. 3b, d). These results demonstrated that T-PVAT transplantation significantly attenuates medial elastin fragmentation and increases collagen deposition of the abdominal aortic wall.
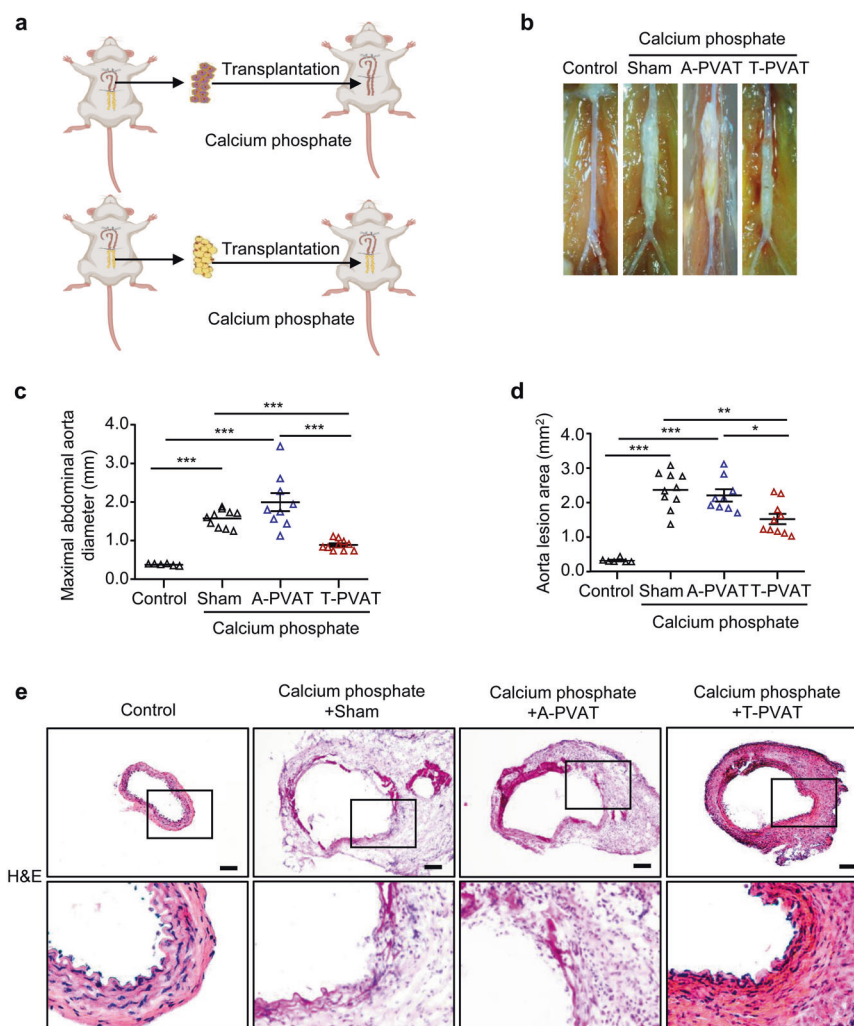
Thoracic PVAT attenuates aortic aneurysm formation
CL Huang et al.

348

Fig. 2 Transplantation of T-PVAT attenuates AAA formation. a Experimental scheme. 8-week-old male C57BL/6 mice were transplanted with isolated T-PVAT and A-PVAT at the infrarenal region of the abdominal aorta, and then undergone calcium phosphate treatment to induce AAA. **b** Representative photographs of abdominal aorta 14 days after $CaPO_4$ treatment with sham control and transplantation of T-PVAT or A-PVAT. **c** Maximal diameter of abdominal aorta. **d** Cross-section lesion area. **e** H&E staining of abdominal aorta. ($n = 6$–10, *$P < 0.05$; **$P < 0.01$; ***$P < 0.001$) (Scale bar = 200 μm).

Transplantation of T-PVAT inhibits macrophage infiltration and MMP-9 production

Macrophage infiltration is one of the most important events in the development and progression of AAA [18]. To examine the effect of T-PVAT transplantation on macrophage infiltration, we stained the abdominal aortic sections with antibody against CD68, a macrophage marker. As shown in Supplementary Fig. S1a, c, abundant accumulation of macrophages was observed in sham group and A-PVAT transplantation group, but not in T-PVAT transplantation group. MMP-9, which is primarily produced by macrophages and plays an important role in matrix destruction [19], was also strikingly elevated in sham group and A-PVAT transplantation group, but not in T-PVAT transplantation group (Supplementary Fig. S1b, d). These results suggest that T-PVAT transplantation inhibits macrophage infiltration and MMP-9 production in the aortic tissues.

Transplantation of T-PVAT preserves smooth muscle cell content in the aortic wall

Smooth muscle cells (SMCs) are a major component of the arterial wall, and a loss of which contributes to degeneration of aortic extracellular matrix (ECM) and subsequent aortic dilation and

rupture [20]. We thus further investigated the content of smooth muscle cell in the aortic wall. Calcium phosphate treatment strongly induced the loss of medial smooth muscle cells in the sham group and A-PVAT transplantation group as indicated by much less alpha-smooth muscle actin (SMA) staining (Fig. 4a, d). However, T-PVAT transplantation significantly increased smooth muscle cell content in the aortic wall. Furthermore, T-PVAT transplantation significantly reduced the expression of apoptosis marker cleaved-caspase3 (Fig. 4b, e) and also TUNEL staining (Fig. 4c, f). All these results suggested that T-PVAT transplantation may inhibit the apoptosis of SMCs and preserves SMC content in the aortic wall.

T-PVAT inhibits VSMC apoptosis

To determine whether T-PVAT has a direct effect on smooth muscle cells, we co-cultured VSMCs with isolated PVAT and then stimulated VSMC with H_2O_2 or TNFα plus cycloheximide (CHX) to induce cell apoptosis. Compared to control or A-PVAT, T-PVAT significantly inhibited H_2O_2- or TNFα plus CHX-induced expression of cleaved-Caspase 3 and cleaved-Parp (Fig. 5a–c, f–h). We further used annexin V assay combined with propidium iodide (PI) staining to distinguish apoptotic cells from necrotic cells by
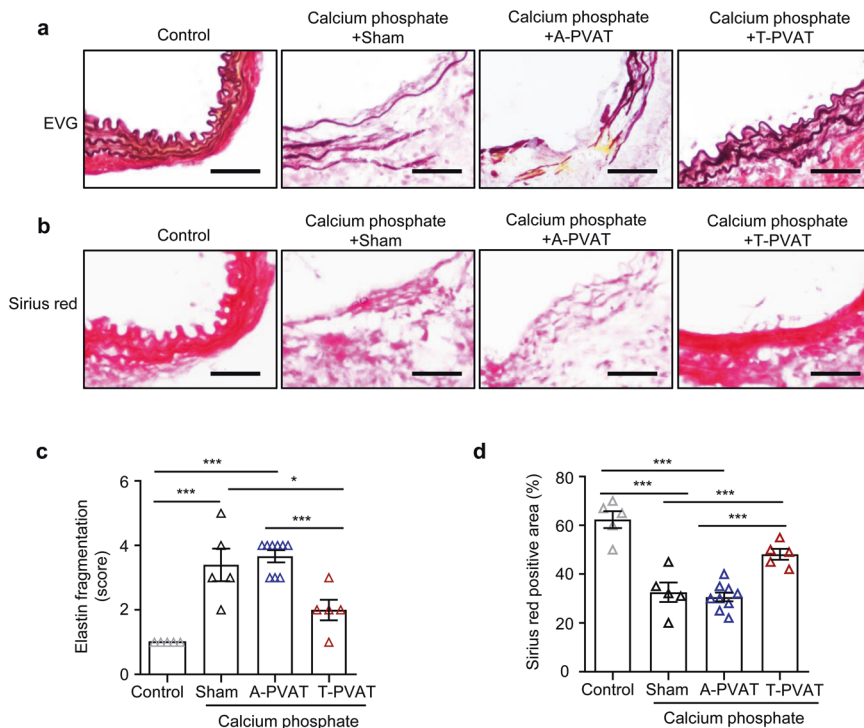
Thoracic PVAT attenuates aortic aneurysm formation
CL Huang et al.

349

Fig. 3 Transplantation of T-PVAT attenuates elastin fragmentation and increases collagen deposition of abdominal aortic wall. **a** Representative image of Elastica Van Gieson (EVG) staining. **b** Representative images of Sirius red staining. **c** Assessment of medial elastica fragmentation. **d** Quantification of Sirius red positive area ($n = 5$–9; *$P < 0.05$; ***$P < 0.001$) (Scale bar = 200 μm).

flow cytometry analysis. T-PVAT significantly inhibited H_2O_2- or TNFα plus CHX-induced apoptosis of VSMCs (Fig. 5d, e, i, j). All these results suggested that T-PVAT can inhibit VSMC apoptosis.

T-PVAT is enriched in browning adipocytes and anti-apoptotic secretory proteins
To understand how T-PVAT exerts its function, an RNA-seq analysis was performed. As shown in Fig. 6a, T-PVAT showed a dramatic difference in gene expression comparing to A-PVAT. A total of 4834 genes were differentially expressed in T-PVAT, including 1609 upregulated and 3225 downregulated (Fig. 6b). The 1609 upregulated genes were then undergoing GO enrichment analysis. As shown in Fig. 6c, the top enriched items were clustered in mitochondrial metabolism and brown fat cell differentiation, which are typical characteristics of browning adipocytes. As growing studies have shown that PVAT exerts its function through endocrine or paracrine ways [5, 7, 17, 21], we then mapped the upregulated DEGs with genes encoding secreted proteins and the overlapped genes were further undergoing enrichment analysis. As shown in Fig. 6d, one of the most significant items enriched from the up regulated secretory proteins were negative regulation of apoptotic process. Taken together, these data suggest that T-PVAT is enriched in browning adipocytes and anti-apoptotic secretory proteins.

The secretome of adipocytes isolated from T-PVAT inhibits VSMC apoptosis
PVAT can be separated into adipocytes and stromal vascular fraction (SVF) which contains immune cells, endothelial cells, fibroblast and adipose stromal cells [22]. To further investigate which component contributes to the anti-apoptotic effect of T-PVAT, we cultured adipocytes and SVF isolated from T-PVAT or A-PVAT and collected the culture medium. We then cultured

VSMCs with these conditioned medium and examined cell apoptosis. As shown in Fig. 7a–c, i–k, culture medium of adipocytes isolated from T-PVAT significantly inhibited H_2O_2- or TNFα plus CHX-induced expression of cleaved-Parp and cleaved-Caspase-3 compared to those from A-PVAT, whereas culture medium from SVF did not have a difference (Fig. 7d–f, l–n). Further, annexin V/PI assay indicated that culture medium of adipocytes isolated from T-PVAT significantly inhibited H_2O_2- or TNFα plus CHX-induced VSMC apoptosis whereas culture medium from SVF did not (Fig. 7g, h, o–p). All these data suggested that T-PVAT exerts its anti-apoptotic effect via the secretome from adipocytes.

Secreted COMP from T-PVAT inhibits VSMC apoptosis
To identify which factor mediates the anti-apoptotic effect of T-PVAT, we integrated RNA-seq data and mass spectrometry data and screened out cartilage oligomeric matrix protein (COMP) as secreted anti-apoptotic protein that is enriched in T-PVAT (Fig. 8a). To confirm this result, we performed a Western blot analysis. As shown in Fig. 8b, COMP expression is significantly higher in the lysates and culture medium of adipocytes derived from T-PVAT than those from A-PVAT. Immunohistochemical staining further confirmed that COMP expression is significantly higher in T-PVAT than in A-PVAT (Fig. 8c).

We then investigated whether COMP exerts an anti-apoptotic effect on VSMCs. As shown in Fig. 8d, e, recombinant COMP protein treatment significantly inhibited TNFα plus CHX-induced VSMC apoptosis. In addition, COMP significantly inhibited the expression of cleaved-Parp and cleaved-Caspase-3 (Fig. 8f–h). As it has previously been suggested that COMP would affect anti-apoptotic factors to increase cell survival [23], we then examined the levels of anti-apoptotic protein Bcl-2 and survivin. As shown in Fig. 8f, i, j, COMP significantly increased survivin protein level while had no effect on Bcl-2 protein level in VSMCs, suggesting that the anti-apoptotic effect of COMP may be mediated by survivin.
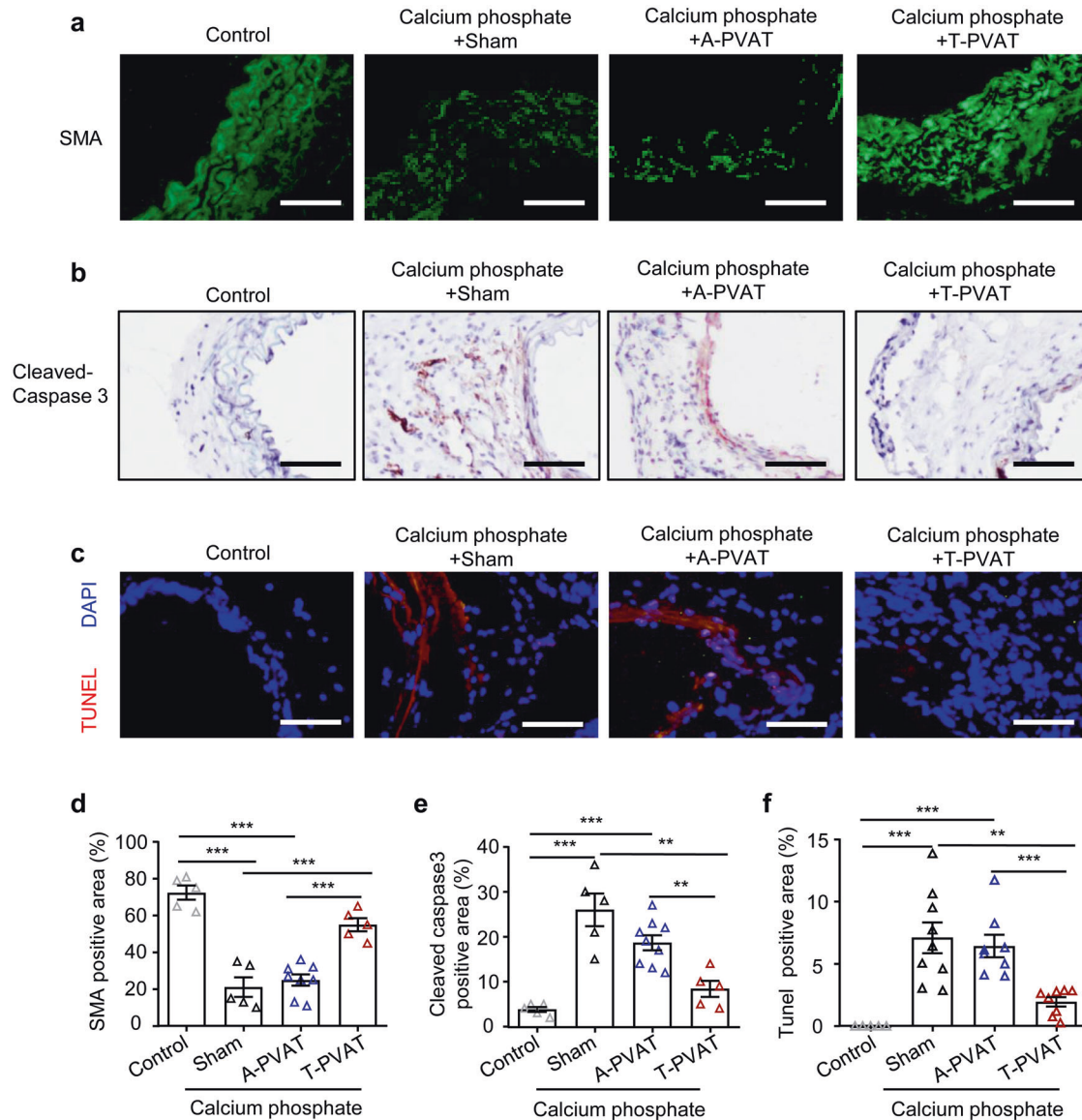
350

Fig. 4 Transplantation of T-PVAT preserves medial smooth muscle cell content in the aortic wall. a Immunofluorescence staining of alpha smooth muscle actin (SMA). **b** Immunohistochemical staining of cleaved Caspase 3. **c** TUNEL staining. **d** Quantification of SMA positive area. **e** Quantification of cleaved-Caspase 3 positive area. **f** Quantification of TUNEL staining ($n = 5-9$; **$P < 0.01$; ***$P < 0.001$) (Scale bar = 200 μm).

DISCUSSION

Here we report that T-PVAT exhibits a more BAT-like phenotype than A-PVAT, and changing the characteristic of PVAT around the abdominal aorta by transplantation of T-PVAT attenuates abdominal aortic aneurysm formation. In addition, T-PVAT inhibits the apoptosis of vascular smooth muscle cells, and this protective effect might be attributed to the anti-apoptotic secretome of T-PVAT.

PVAT had traditionally been thought to simply provide structural support for blood vessels. However, recent evidence also links PVAT to vascular homeostasis and pathogenesis. Accumulating data suggest that PVAT plays an important role in atherosclerosis and hypertension [4, 5, 8, 9]. Recently PVAT has also been linked to nonatherosclerotic vascular diseases such as AAA. Greater amounts of PVAT were found to be associated with AAA development [24, 25]. PVAT-derived growth factors such as PDGF-D and leptin contributed to aortic aneurysm formation during obesity [11, 12], whereas adiponectin, which is produced almost exclusively by the adipose tissue and downregulated in obesity, protected against AAA formation and growth [26]. These studies suggest that both PVAT quantity and quality are closely associated with AAA development. However, currently there is no direct evidence of PVAT involvement in AAA. Here we showed that T-PVAT was dramatically different from A-PVAT, with a much more BAT-like and anti-apoptotic feature. Change of PVAT around the abdominal aorta by transplantation of T-PVAT significantly prevents calcium phosphate-induced AAA formation. To the best of our knowledge, this is the first time to show that different types of PVAT may have direct impact on aortic aneurysm formation. Our results suggest that changing the characteristics of PVAT, especially by enhancing its browning, may have therapeutic potential in AAA prevention or management.
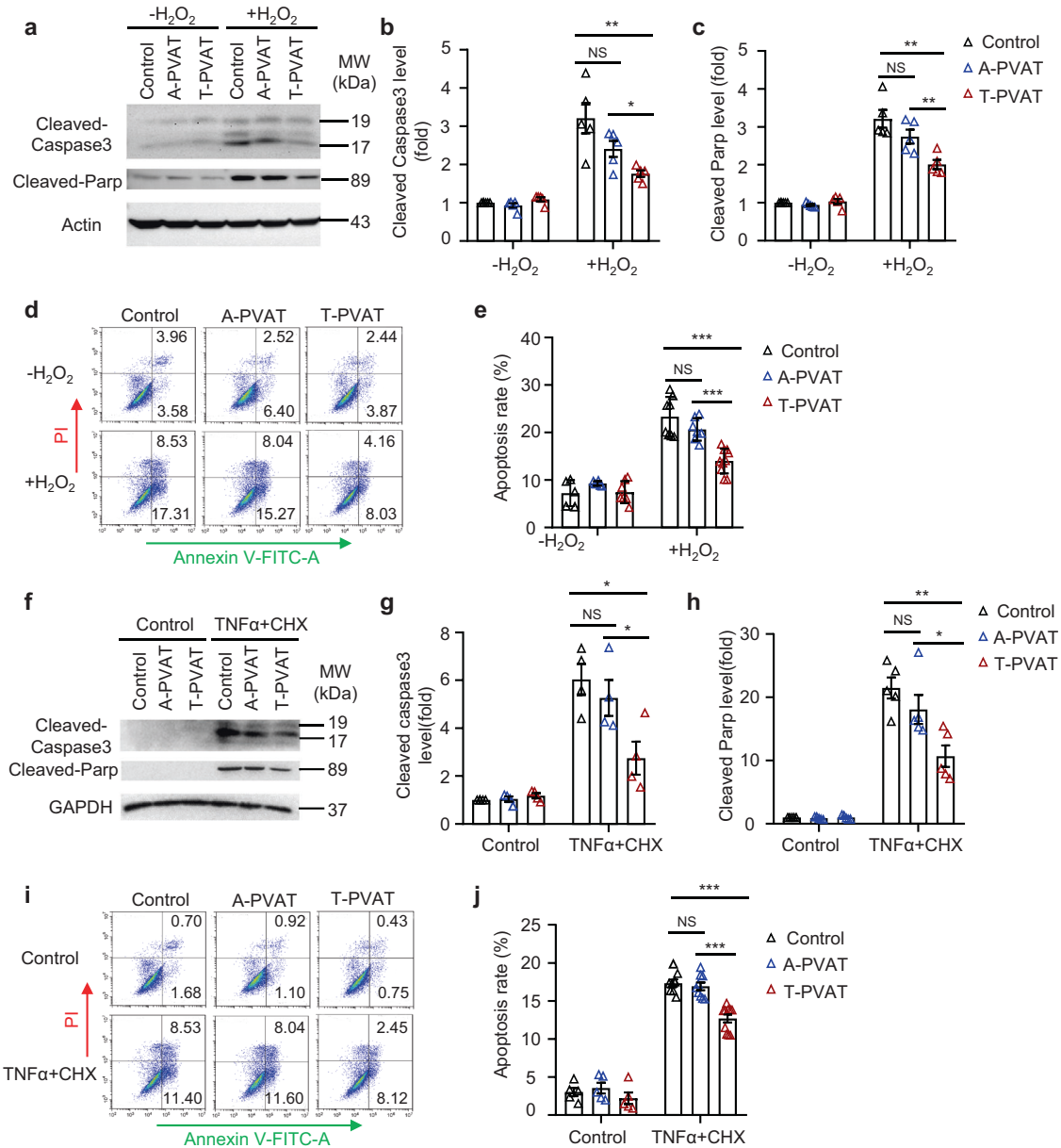
Thoracic PVAT attenuates aortic aneurysm formation
CL Huang et al.

351

Fig. 5 Co-culture of T-PVAT inhibits VSMC apoptosis. Primary VSMCs were co-cultured with/without A-TVAT or T-PVAT for 24 h and then treated with 400 μM H_2O_2 for 24 h (**a–e**) or 50 ng/mL TNFα plus 5 μg/mL cycloheximide for 8 h (**f–j**). **a**, **f** Representative images of Western blotting analysis. **b**, **g** Quantification of cleaved-Caspase 3. **c**, **h** Quantification of cleaved-Parp. **d**, **i** Annexin V/PI staining and flow cytometry analysis. **e**, **j** Percentage of apoptotic cells (Annexin V$^+$) ($n = 4$–10; *$P < 0.05$; **$P < 0.01$; ***$P < 0.001$; NS not significant).

Similar to adipose tissue in other depots, PVAT is also recognized as an active endocrine tissue. However, there are substantial differences between the secretomes from brown and white adipocytes [27]. Previously a full genome DNA microarray analysis has revealed that global gene expression profiles of T-PVAT are virtually identical to BAT, with equally high expression of Ucp1 and other genes known to be uniquely or very highly expressed in BAT [28], which is consistent with our findings that T-PVAT is a much more BAT-like tissue than A-PVAT. Therefore, it is conceivable that different secretomes from T-PVAT and A-PVAT might contribute to their different effects on smooth muscle cells and AAA formation. Indeed, our co-culture experiment revealed that isolated T-PVAT can inhibit the apoptosis of VSMCs. In addition, RNA-seq data

indicated that T-PVAT is enriched in anti-apoptotic secretory proteins compared to A-PVAT. However, PVAT is composed of adipocytes and stromal vascular fraction (SVF) which contains immune cells, endothelial cells, fibroblast and adipose stromal cells. We further verified that adipocyte-, but not SVF-derived conditioned medium from T-PVAT significantly inhibits VSMC apoptosis compared to those from A-PVAT. These data suggest that different secretomes of PVAT with different browning extent may have a direct impact on vascular homeostasis and the development of aortic aneurysm formation.

In conclusion, our study demonstrates that T-PVAT is more BAT-like than A-PVAT, and transplantation of T-PVAT inhibits VSMC apoptosis and AAA formation, which is possible through paracrine
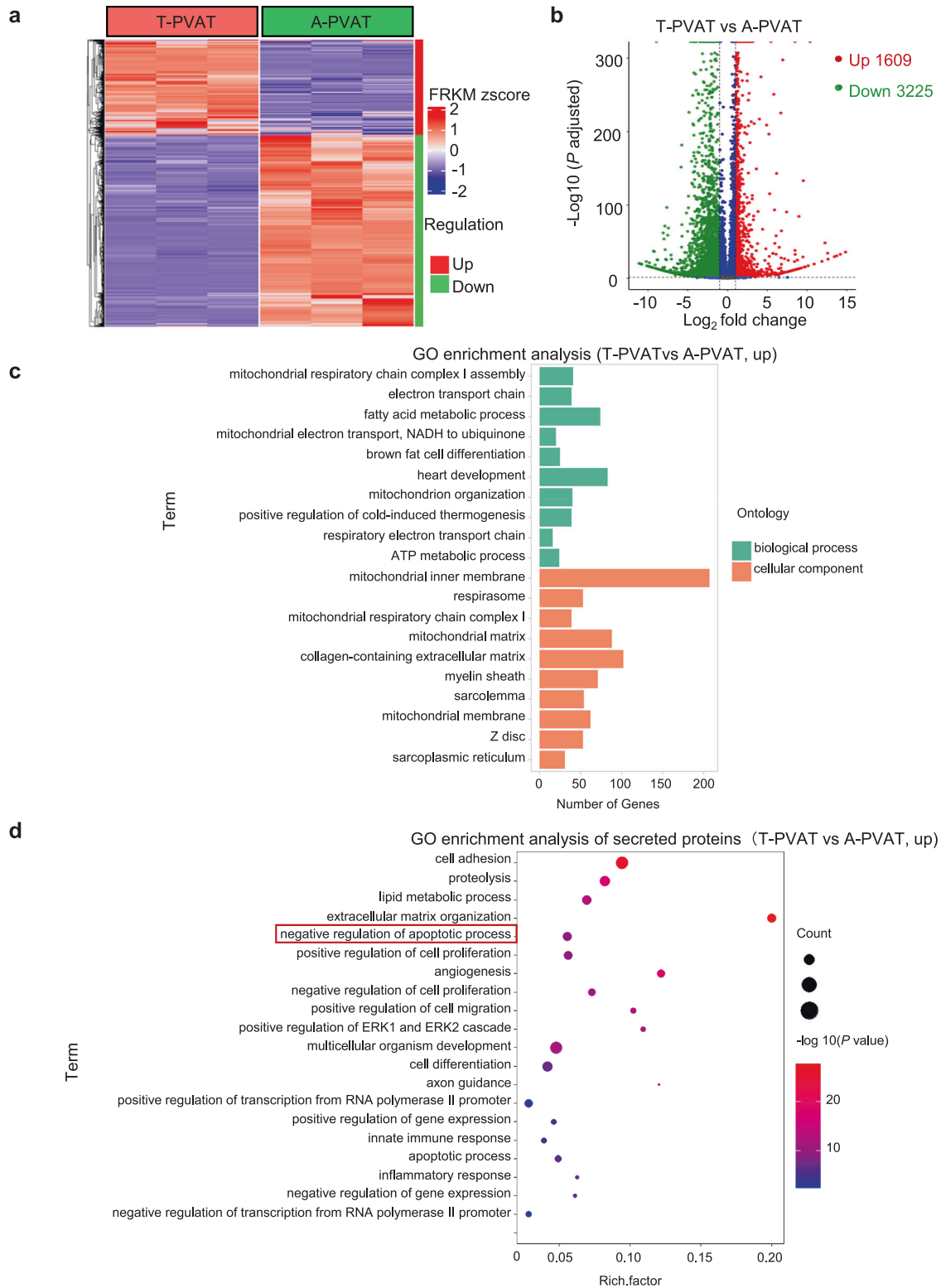
Thoracic PVAT attenuates aortic aneurysm formation
CL Huang et al.

352

Fig. 6 T-PVAT is enriched in browning adipocytes and anti-apoptotic secretory proteins. a Heatmap of differentially expressed genes (DEGs) from RNA-seq data. **b** Volcano plot from RNA-seq data. **c** GO enrichment analysis for the DEGs. **d** Top 20 biological processes for the upregulated secreted proteins. The circle size represents the gene number. The color gradient shows the adjusted P value ($n = 3$).
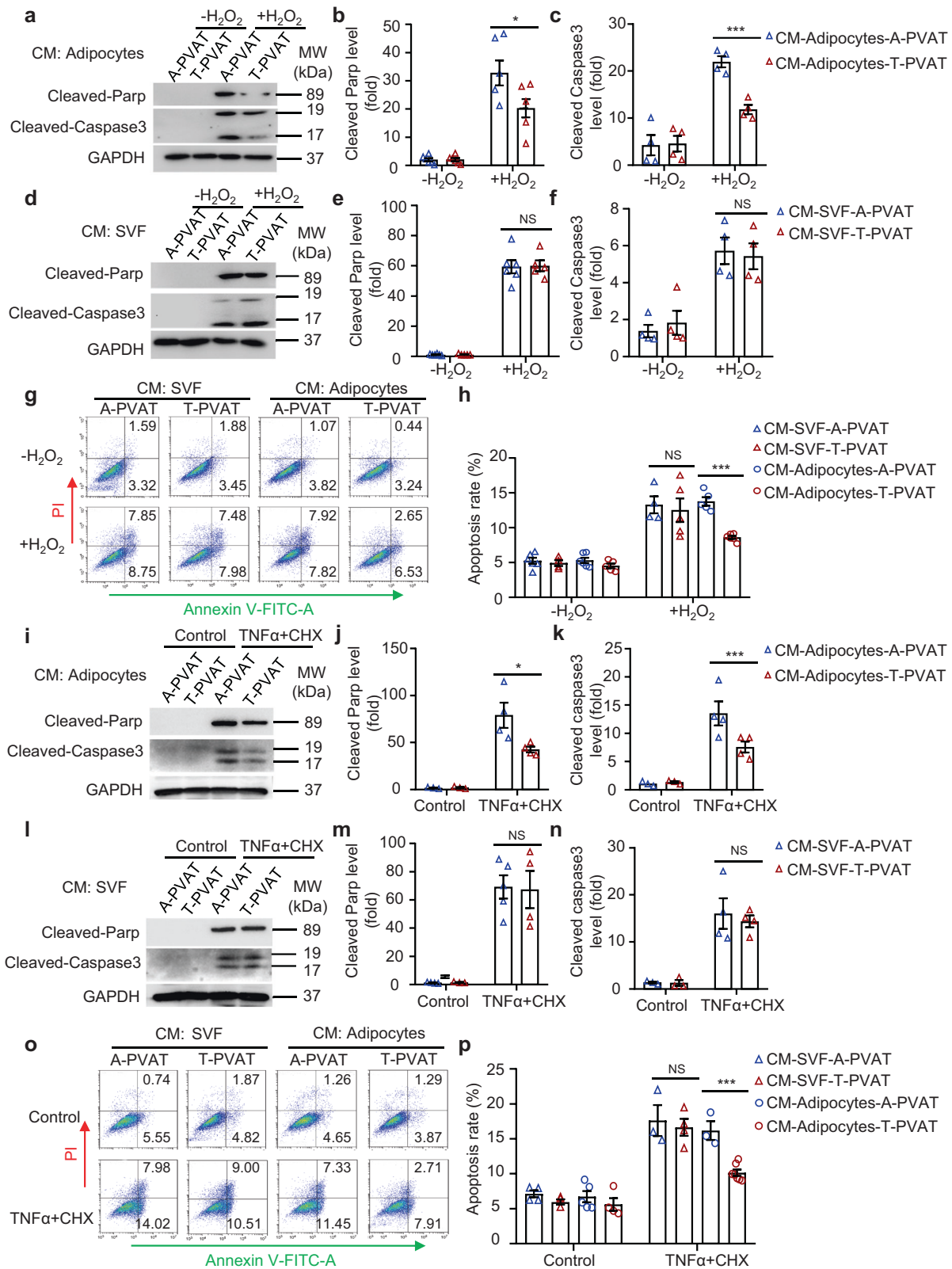
Thoracic PVAT attenuates aortic aneurysm formation
CL Huang et al.

353

Fig. 7 The secretome of adipocytes isolated from T-PVAT inhibits VSMC apoptosis. Primary VSMCs were cultured with conditioned medium collected from adipocytes and SVF that were isolated from T-PVAT or A-PVAT, and then cells were treated with 400 μM H_2O_2 for 24 h (**a–h**) or 50 ng/mL TNFα plus 5 μg/mL cycloheximide for 8 h (**i–p**). **a, d, i, l** Representative images of Western blotting analysis. **b, e, j, m** Quantification of cleaved-Parp. **c, f, k, n** Quantification of cleaved-Caspase 3. **g, o** Annexin V/PI staining and flow cytometry analysis. **h, p** Percentage of apoptotic cells (Annexin V^+) ($n = 3$–6; $*P < 0.05$; $***P < 0.001$; NS not significant).

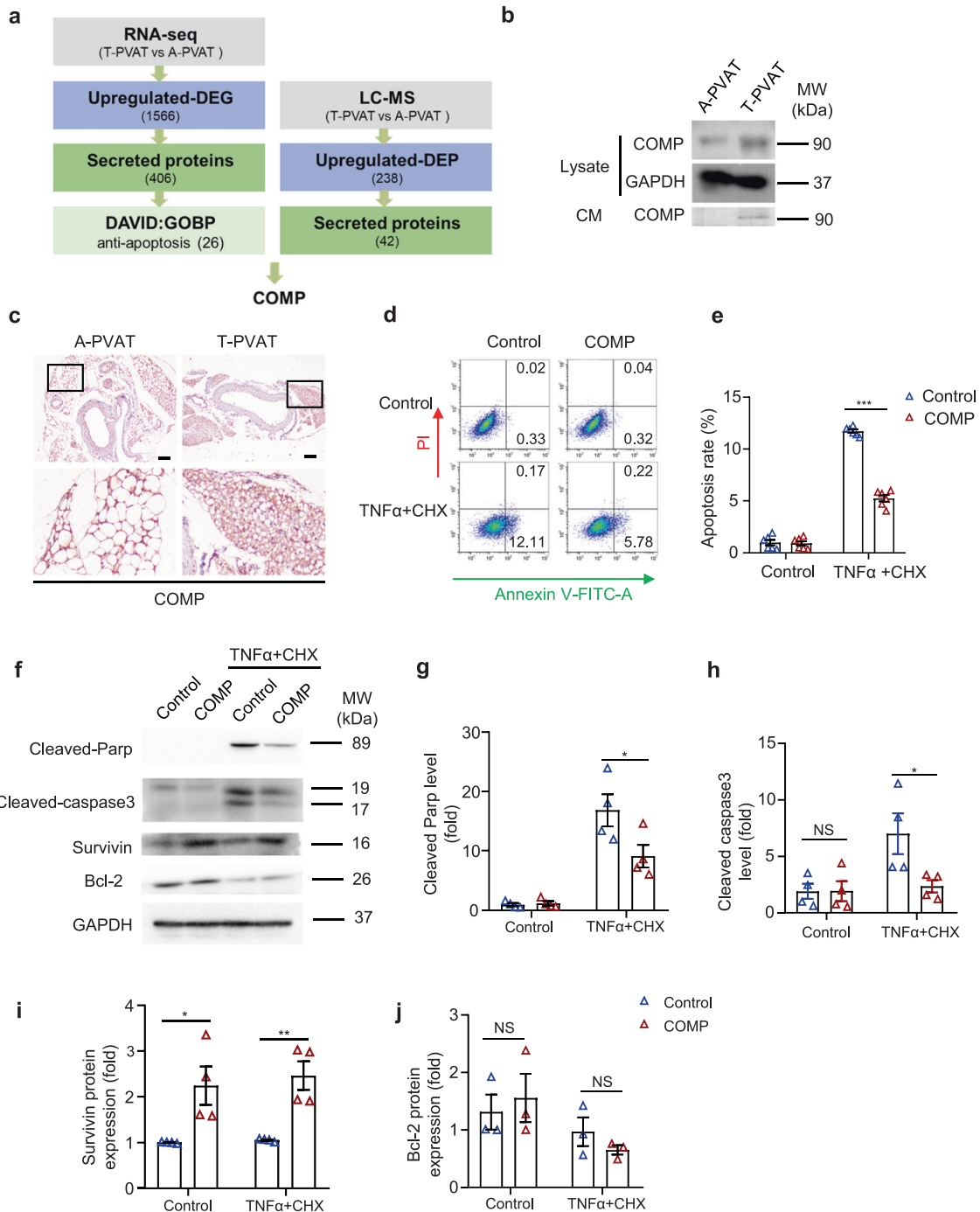Thoracic PVAT attenuates aortic aneurysm formation
CL Huang et al.

354

Fig. 8 Secreted COMP from T-PVAT inhibits VSMC apoptosis. a Screening scheme. **b** Western blotting analysis of COMP expression in the lysates and culture medium of adipocytes derived from A-PVAT and T-PVAT (three independent repeated experiments were performed). **c** Immunohistochemical staining of COMP. **d** Annexin V/PI staining and flow cytometry analysis. **e** Percentage of apoptotic cells (Annexin V+). **f** Representative images of Western blotting analysis. **g** Quantification of cleaved-Parp. **h** Quantification of cleaved-Caspase 3. **i** Quantification of survivin. **j** Quantification of Bcl-2 ($n = 3–6$; *$P < 0.05$; **$P < 0.01$; ***$P < 0.001$; NS not significant).

or endocrine effects. These observations provide a potential novel therapeutic approach for AAA.

AUTHOR CONTRIBUTIONS
ZYL, YXC and JFW directed the project. ZYL designed the experiments and drafted the manuscript. CLH, YNH, and LY, JPL, ZHZ, ZQH, SXC performed the experiments and analyzed the data. YLZ helped with data curation.

Thoracic PVAT attenuates aortic aneurysm formation
CL Huang et al.

355

ADDITIONAL INFORMATION

REFERENCES

1. Howard DP, Banerjee A, Fairhead JF, Handa A, Silver LE, Rothwell PM, et al. Population-based study of incidence of acute abdominal aortic aneurysms with projected impact of screening strategy. J Am Heart Assoc. 2015;4:e001926.
2. Chang L, Garcia-Barrio MT, Chen YE. Perivascular adipose tissue regulates vascular function by targeting vascular smooth muscle cells. Arterioscler Thromb Vasc Biol. 2020;40:1094–109.
3. Soltis EE, Cassis LA. Influence of perivascular adipose tissue on rat aortic smooth muscle responsiveness. Clin Exp Hypertens A. 1991;13:277–96.
4. Verlohren S, Dubrovska G, Tsang SY, Essin K, Luft FC, Huang Y, et al. Visceral periadventitial adipose tissue regulates arterial tone of mesenteric arteries. Hypertension. 2004;44:271–6.
5. Lee YC, Chang HH, Chiang CL, Liu CH, Yeh JI, Chen MF, et al. Role of perivascular adipose tissue-derived methyl palmitate in vascular tone regulation and pathogenesis of hypertension. Circulation. 2011;124:1160–71.
6. Manka D, Chatterjee TK, Stoll LL, Basford JE, Konaniah ES, Srinivasan R, et al. Transplanted perivascular adipose tissue accelerates injury-induced neointimal hyperplasia: role of monocyte chemoattractant protein-1. Arterioscler Thromb Vasc Biol. 2014;34:1723–30.
7. Schroeter MR, Eschholz N, Herzberg S, Jerchel I, Leifheit-Nestler M, Czepluch FS, et al. Leptin-dependent and leptin-independent paracrine effects of perivascular adipose tissue on neointima formation. Arterioscler Thromb Vasc Biol. 2013;33:980–7.
8. Chang L, Villacorta L, Li R, Hamblin M, Xu W, Dou C, et al. Loss of perivascular adipose tissue on peroxisome proliferator-activated receptor-gamma deletion in smooth muscle cells impairs intravascular thermoregulation and enhances atherosclerosis. Circulation. 2012;126:1067–78.
9. Verhagen SN, Vink A, van der Graaf Y, Visseren FL. Coronary perivascular adipose tissue characteristics are related to atherosclerotic plaque size and composition. A post-mortem study. Atherosclerosis. 2012;225:99–104.
10. Meekel JP, Dias-Neto M, Bogunovic N, Conceicao G, Sousa-Mendes C, Stoll GR, et al. Inflammatory gene expression of human perivascular adipose tissue in abdominal aortic aneurysms. Eur J Vasc Endovasc Surg. 2021;61:1008–16.
11. Liu CL, Ren J, Wang Y, Zhang X, Sukhova GK, Liao M, et al. Adipocytes promote interleukin-18 binding to its receptors during abdominal aortic aneurysm formation in mice. Eur Heart J. 2019;41:2456–68.
12. Zhang ZB, Ruan CC, Lin JR, Xu L, Chen XH, Du YN, et al. Perivascular adipose tissue-derived PDGF-D contributes to aortic aneurysm formation during obesity. Diabetes. 2018;67:1549–60.
13. Padilla J, Jenkins NT, Vieira-Potter VJ, Laughlin MH. Divergent phenotype of rat thoracic and abdominal perivascular adipose tissues. Am J Physiol Regul Integr Comp Physiol. 2013;304:R543–52.
14. Isselbacher EM. Thoracic and abdominal aortic aneurysms. Circulation. 2005;111:816–28.
15. Mathur A, Mohan V, Ameta D, Gaurav B, Haranahalli P. Aortic aneurysm. J Transl Int Med. 2016;4:35–41.
16. Yamanouchi D, Morgan S, Stair C, Seedial S, Lengfeld J, Kent KC, et al. Accelerated aneurysmal dilation associated with apoptosis and inflammation in a newly developed calcium phosphate rodent abdominal aortic aneurysm model. J Vasc Surg. 2012;56:455–61.
17. Takaoka M, Nagata D, Kihara S, Shimomura I, Kimura Y, Tabata Y, et al. Periadventitial adipose tissue plays a critical role in vascular remodeling. Circ Res. 2009;105:906–11.
18. Raffort J, Lareyre F, Clement M, Hassen-Khodja R, Chinetti G, Mallat Z. Monocytes and macrophages in abdominal aortic aneurysm. Nat Rev Cardiol. 2017;14:457–71.
19. Longo GM, Xiong W, Greiner TC, Zhao Y, Fiotti N, Baxter BT. Matrix metalloproteinases 2 and 9 work in concert to produce aortic aneurysms. J Clin Invest. 2002;110:625–32.
20. Quintana RA, Taylor WR. Cellular mechanisms of aortic aneurysm formation. Circ Res. 2019;124:607–18.
21. Li X, Ballantyne LL, Yu Y, Funk CD. Perivascular adipose tissue-derived extracellular vesicle miR-221-3p mediates vascular remodeling. FASEB J: Off Publ Federation Am Societies Exp Biol. 2019;33:12704–22.
22. Szasz T, Webb RC. Perivascular adipose tissue: more than just structural support. Clin Sci. 2012;122:1–12.
23. Gagarina V, Carlberg AL, Pereira-Mouries L, Hall DJ. Cartilage oligomeric matrix protein protects cells against death by elevating members of the IAP family of survival proteins. J Biol Chem. 2008;283:648–59.
24. Dias-Neto M, Meekel JP, van Schaik TG, Hoozemans J, Sousa-Nunes F, Henriques-Coelho T, et al. High density of periaortic adipose tissue in abdominal aortic aneurysm. Eur J Vasc Endovasc Surg. 2018;56:663–71.
25. Thanigaimani S, Golledge J. Role of adipokines and perivascular adipose tissue in abdominal aortic aneurysm: a systematic review and meta-analysis of animal and human observational studies. Front Endocrinol (Lausanne). 2021;12:618434.
26. Yoshida S, Fuster JJ, Walsh K. Adiponectin attenuates abdominal aortic aneurysm formation in hyperlipidemic mice. Atherosclerosis. 2014;235:339–46.
27. Deshmukh AS, Peijs L, Beaudry JL, Jespersen NZ, Nielsen CH, Ma T, et al. Proteomics-based comparative mapping of the secretomes of human brown and white adipocytes reveals EPDR1 as a novel batokine. Cell Metab. 2019;30:963–75.e7.
28. Fitzgibbons TP, Kogan S, Aouadi M, Hendricks GM, Straubhaar J, Czech MP. Similarity of mouse perivascular and brown adipose tissues and their resistance to diet-induced inflammation. Am J Physiol Heart Circ Physiol. 2011;301:H1425–37.